

Wireless LAN for IoT 5G applications in a congested indoor environment: improved primary signal sensing at millimeter-wave V-band [40 - 75 GHz]

H. E. ADARDOUR^{1,3*}, S. KAMECHE^{2,3}

¹ Department of Electronics, Faculty of Technology, University Hassiba Benbouali, Chlef, Algeria - h.adardour@univ-chlef.dz

² Department of Telecommunications, Faculty of Technology, University Abou Bekr Belkaid, Tlemcen, Algeria –samir.kameche@univ-tlemcen.dz

³ STIC Laboratory, Faculty of Technology, University Abou Bekr Belkaid, Tlemcen, Algeria

KEY WORDS: 5G, 60 GHz, mm-Waves, IoT, GMRMM, SER, SED.

ABSTRACT:

Presently, the IEEE 802.11ad wireless network standard supports the communication capability within the V band of millimeter-Waves (or mm-Waves) [40 – 75 GHz] for Internet of Things (or IoT) technology. This paper presents an algorithm to improve the Primary Signal 5G (or PS_{5G}) sensing at 60 GHz in WLAN_{IoT-5G} (or Wireless Local Area Network for IoT-5G). To achieve that, we aim at investigating and assessing the sensing performances of the PS_{5G} from the Access Point of WLAN_{IoT-5G} (or APWLAN_{IoT-5G}) by the Secondary User IoT-5G (or SU_{IoT-5G}) in a congested environment using a simple energy detector (or SED) algorithm and a simple recursive estimator (or SRE). In addition, the SU_{IoT-5G} is regarded as a mobile user in WLAN_{IoT-5G} by employing the Gauss-Markov Random Mobility Model (or GMRMM). Through various scenario simulations, the performances and the robustness of the proposed algorithm are proved.

1. INTRODUCTION

The arrival of next-generation cellular communications, or 5G technology, promises to be a great development for the Internet of Things (or IoT) industry. Besides, the deployment of the 5G network will strongly contribute to increasing the capability and reliability of IoT devices. With the growth of the IoT accelerating over the last few years, it has been necessary to develop innovative solutions. However, these solutions aim to multiply the amount of data that can be transmitted as well as its throughput. This will ensure that the current infrastructures can meet the expected increase in connected devices and data transmission. The implementation of 5G wireless mobile internet technology is one of the most modern solutions available to address this problem (Azzahra et al., 2017; Singh et al., 2018; Herschfelt et al., 2021; Mohanty et al., 2021; objetconnecte. net., 2022, S. Date: 30.06.2022).

The commercial success of any IoT device relies on its performance. It depends on how well a device can communicate with other IoT devices, smartphones, and tablets, as well as software in the form of apps or websites, etc. Under 5G technology, the data transfer rates are rising dramatically. 5G technology has up to 10 more data rates than the older 4G technology. This throughput improvement enables all IoT devices the ability to communicate and share data more efficiently than ever before (Azzahra et al., 2017; Singh et al., 2018; Herschfelt et al., 2021; Mohanty et al., 2021; objetconnecte. net., 2022, S. Date: 30.06.2022).

Wireless Local Area Networks (or WLANs) are founded on a standard that constitutes the integrated solutions suitable for networking in such a way that offers mobility, flexibility, installation ease, and low cost for the implementation of the 5G wireless IoT technology (Azzahra et al., 2017; Singh et al., 2018; Herschfelt et al., 2021; Mohanty et al., 2021; objetconnecte. net., 2022, S. Date: 30.06.2022).

The application of millimeter-Waves (or mm-Waves) is an attractive solution for higher data rates (or Gbps) in short-range

applications. However, mm-Waves are extremely vulnerable to propagation losses and various obstacles such as furniture and walls. Therefore, the growing need for higher frequencies has caused many scientists to prioritize mm-Waves at 60 GHz. The 60 GHz band is a good prospect for future high-speed WLAN-IoT communication systems, it offers a cost and time advantage for the device manufacturers to guarantee the quality of the consumers (Azzahra et al., 2017; Singh et al., 2018; Herschfelt et al., 2021; Mohanty et al., 2021; objetconnecte. net., 2022, S. Date: 30.06.2022).

The vast portion of the spectrum available at the 60 GHz band is freely accessible throughout the world, which explains the emergence of new technology allowing Wi-Fi connections. This license-free spectrum is more suitable for higher frequency bands such as mm-Waves bands and it contributes significantly to the improvement of users' living quality (Azzahra et al., 2017; Singh et al., 2018; Herschfelt et al., 2021; Mohanty et al., 2021; objetconnecte. net., 2022, S. Date: 30.06.2022).

Recently, the mm-Wave (or 5G) spectrum sensing problems in WLAN_{IoT-5G} have been widely reported in the literature. This article outlines a new approach to improve the spectrum sensing reliability in WLAN_{IoT-5G}. A key challenge in WLAN_{IoT-5G} is to detect all the information about the Secondary User IoT-5G (or SU_{IoT-5G}), when it is moving, particularly in a congested environment, as the mobility of this user (or SU_{IoT-5G}) has a considerable impact on the sensing performances of the Access Point of WLAN_{IoT-5G} (or APWLAN_{IoT-5G}). So, an algorithm is proposed which provides a high detection level, for a SU_{IoT-5G} moving at low speed in a congested environment. Furthermore, the shading element becomes significant in a congested environment. Thus, a weighted average mechanism is needed to achieve a stable measure of the signal strength at the SU_{IoT-5G}. To achieve this, a simple recursive estimator (or SRE) is performed. In the end, the proposed algorithm is evaluated through simulations and results using MATLAB 2017a.

Nevertheless, the proposed algorithm map in this paper is shown in Fig. 1 with two implementation phases:

The first phase relies on three steps to complete it, such as:

- First step: In this work, the mobility model to be employed for the SU_{IoT-5G} is the Gauss-Markov Random Mobility Model (or GMRMM) (Liang et al., 1999; Xiaoyan et al., 1999; Tracy et al., 2002; Geng et al., 2013).
- Second step: Regarding the propagation models, one must employ the Log-Normal Shading model (or LNS) with LOS and NLOS, to predict the received signal strength at the SU_{IoT-5G} (Othmane and Adnane, 2020).
- Third step: After the received signal strength 5G (or RSS_{5G}) at the SU_{IoT-5G} is predicted in a congested

environment, one will rely on a SRE for estimating the RSS_{5G} at the SU_{IoT-5G} with higher and better measurement stability. Next, one can estimate the signal-to-noise ratio (or SNR) link between the $APWLAN_{IoT-5G}$ and the SU_{IoT-5G} (Adardour et al., 2017).

Concerning the second phase:

To authenticate the detection level of the transmitted primary signal 5G (or PS_{5G}) at 60 GHz from the $APWLAN_{IoT-5G}$, a simple energy detector (or SED) is exploited by the SU_{IoT-5G} (Adardour et al., 2015).

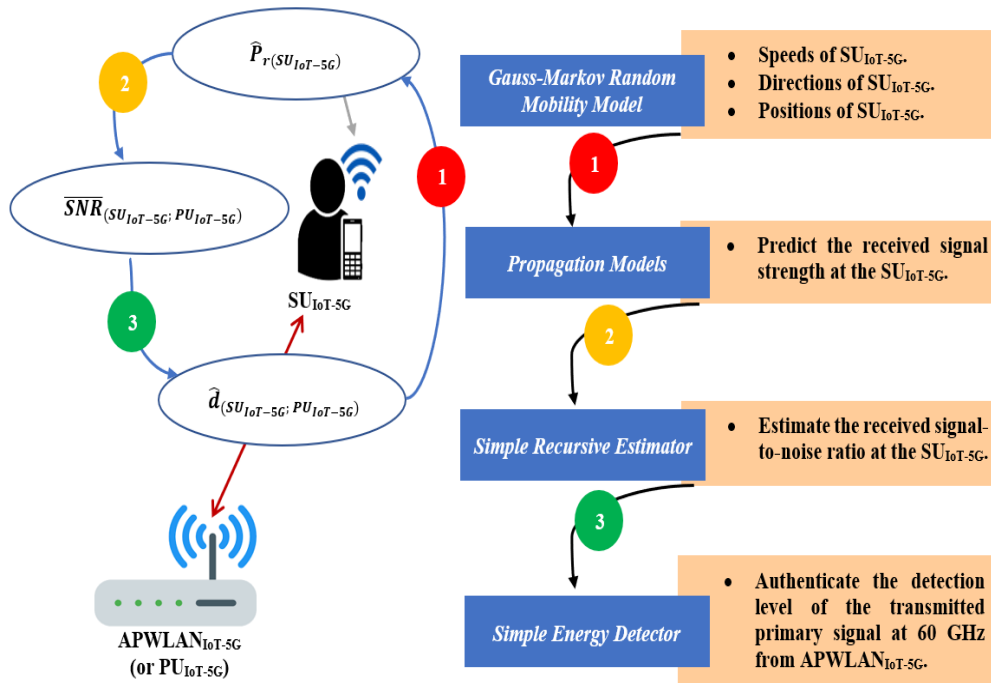


Figure 1. Proposed algorithm map: PS_{5G} sensing cycle.

For achieving the intended goal, the present research consists of three sections that follow a general introduction to the 60 GHz IoT technology. In section 2, we discuss the proposed algorithm. The simulation and the obtained results are shown and discussed in Section 3. Finally, we report some conclusions in Section 4.

2. PROPOSED ALGORITHM

2.1 Gauss-Markov random mobility model

In wireless communication applications, the RSS_{5G} corresponds to a measurement of the signal reception power 5G (or RSP_{5G}) outdoors or indoors wireless. This is typically applied in RF (or Radio-Frequency) for determining the estimated position of a user node (here it is the SU_{IoT-5G}) or the estimated distance between two nodes, i.e., the SU_{IoT-5G} and the reference node (here it is the $APWLAN_{IoT-5G}$). In the literature, however, there are various algorithms for a mobility model that can be employed to estimate the node position (here it is the SU_{IoT-5G}) for any moving. For further information please consult references (Liang et al., 1999; Xiaoyan et al., 1999; Tracy et al., 2002; Geng et al., 2013).

A mobility model aims to depict the motion pattern of the SU_{IoT-5G} node, which includes its true position, velocity, and direction over time. The examined and studied model in this research is the Gauss-Markov random mobility model (or GMRMM). The GMRMM was firstly presented by the authors, Liang and Haas, in 1999. It was aimed at the analysis of a mobile wireless communication node in PCSNs (or personal communication services networks). It has been largely applicable, especially in ad-hoc networks (Tracy et al., 2002; Geng et al., 2013).

However, the purpose of the first step would be to estimate the position of the SU_{IoT-5G} node moving in the $APWLAN_{IoT-5G}$ coverage area. Then, the link distance from the SU_{IoT-5G} node to the $APWLAN_{IoT-5G}$ node is estimated and applied in the second step. The details of the chosen model are presented in this subsection. An alternative representation of the GMRMM is based on the following state equations (Tracy et al., 2002; Geng et al., 2013):

$$\begin{aligned}
 V_{SU_{10T-5G}}(t) &= \alpha \cdot V_{SU_{10T-5G}}(t-1) + (1 - \alpha) \cdot \bar{V}_{SU_{10T-5G}} + \dots \\
 &\quad \dots + (\sqrt{1 - \alpha^2}) \cdot W_{V_{SU_{10T-5G}}(t-1)} \\
 D_{SU_{10T-5G}}(t) &= \alpha \cdot D_{SU_{10T-5G}}(t-1) + (1 - \alpha) \cdot \bar{D}_{SU_{10T-5G}} + \dots \\
 &\quad \dots + (\sqrt{1 - \alpha^2}) \cdot W_{D_{SU_{10T-5G}}(t-1)}
 \end{aligned} \quad (1)$$

Where $V_{SU_{10T-5G}}(t)$ and $D_{SU_{10T-5G}}(t)$ denote the velocity and direction of the path of the SU_{10T-5G} node, respectively, at time t , $\bar{V}_{SU_{10T-5G}}$ and $\bar{D}_{SU_{10T-5G}}$ are constants indicating the average values of velocity and direction, respectively, and, $W_{V_{SU_{10T-5G}}(t-1)}$ and $W_{D_{SU_{10T-5G}}(t-1)}$ are consistent with random variables pertaining to a Gaussian distribution of mean zero and standard deviation σ . The GMRMM randomness is produced by means of a configuration setting α ($0 < \alpha \leq 1$).

At each time interval, the targeted position of the SU_{10T-5G} node may be derived from its actual velocity and direction of motion. More conveniently, assuming that the SU_{10T-5G} node is moving along the X and Y axes, then at the instant t of the interval, its position may be determined using the following state equations (Tracy et al., 2002; Geng et al., 2013):

$$\begin{aligned}
 x_{SU_{10T-5G}}(t) &= x_{SU_{10T-5G}}(t-1) + \dots \\
 &\quad \dots + V_{SU_{10T-5G}}(t-1) \cdot \cos(D_{SU_{10T-5G}}(t-1)) \\
 y_{SU_{10T-5G}}(t) &= y_{SU_{10T-5G}}(t-1) + \dots \\
 &\quad \dots + V_{SU_{10T-5G}}(t-1) \cdot \sin(D_{SU_{10T-5G}}(t-1))
 \end{aligned} \quad (2)$$

Where, $(x_{SU_{10T-5G}}(t), y_{SU_{10T-5G}}(t))$ and $(x_{SU_{10T-5G}}(t-1), y_{SU_{10T-5G}}(t-1))$ are the coordinates at instants t and $(t - 1)$, respectively; $D_{SU_{10T-5G}}(t-1)$ and $V_{SU_{10T-5G}}(t-1)$ are the direction and velocity of the SU_{10T-5G} , respectively, at instants $(t - 1)$.

2.2 SNR sensitivity and simple recursive estimator

The mobile tracking (here it is the SU_{10T-5G}) in wireless communication networks based on radio frequencies, is often done with the help of the RSS_{5G} , which is applied to estimate the distance from a mobile node (here it is the SU_{10T-5G}) to an access point node (here it is the $APWLAN_{10T-5G}$). When using RF to track mobile node (here it is the SU_{10T-5G}) and estimate distances (SU_{10T-5G} node to $APWLAN_{10T-5G}$ node), some challenges must be addressed, such as signal attenuation, noise, multipath effects, physical obstacles, temperature effect, and so on. On account of these difficulties and the interference with other received signals, the PS_{5G} sensing is becoming difficult. Furthermore, the objective of this second step is to predict the RSS_{5G} at the receiver (or SU_{10T-5G}) and then employ it in the third step in order to estimate the SNR from the transmitter (or $APWLAN_{10T-5G}$) to the receiver (or SU_{10T-5G}), for each distance linking them, as illustrated in Fig. 1 (Othmane et al., 2020; Adardour et al., 2017).

In this sub-section, we describe the estimation method that has been applied in the proposed $WLAN_{10T-5G}$ model. The major elements of the estimation method are summarized in Table 1.

At first, the $WLAN_{10T-5G}$ model is trained by the $APWLAN_{10T-5G}$ and the SU_{10T-5G} , and the critical parameter that separates the $APWLAN_{10T-5G}$ and the SU_{10T-5G} is the sensing channel, where the PS_{5G} is propagated. Furthermore, the current channel condition should be evaluated by the SNR sensitivity ($\overline{SNR}_{(SU_{10T-5G}; PU_{10T-5G})}$) at each link from $APWLAN_{10T-5G}$ to SU_{10T-5G} (see Fig. 1). Consequently, the sensitivity assessment of the $\overline{SNR}_{(SU_{10T-5G}; PU_{10T-5G})}$ must use parameters such as: the

estimated distance ($\hat{d}_{(SU_{10T-5G}; PU_{10T-5G})}$) between the SU_{10T-5G} and the $APWLAN_{10T-5G}$, the estimate of ($\hat{P}_r(SU_{10T-5G})$) at the SU_{10T-5G} , and the noise power (N_{Power}). However, as the SU_{10T-5G} moves around a congested environment, there is a need for a weighted averaging mechanism to produce a consistent measure of the RSS_{5G} at the SU_{10T-5G} . This is achieved using a simple recursive estimator (or SRE). The estimation method is as follows:

<p>For $(x_0(SU_{10T-5G}), y_0(SU_{10T-5G}))$ to $(x_i(SU_{10T-5G}), y_j(SU_{10T-5G}))$, do:</p> <ol style="list-style-type: none"> 1. Estimate the distance from SU_{10T-5G} to PU_{10T-5G} ($\hat{d}_{(SU_{10T-5G}; PU_{10T-5G})}$); 2. Estimate the RSS_{5G} at the SU_{10T-5G} ($\hat{P}_r(SU_{10T-5G})$); 3. Estimate the sensitivity of the $\overline{SNR}_{(SU_{10T-5G}; PU_{10T-5G})}$ between the SU_{10T-5G} and the PU_{10T-5G}. <p>End for</p>
--

Table 1. Estimating method.

2.2.1 Distance estimating: The Euclidean distance in [m] can be used to compute the estimated distance from two nodes the SU_{10T-5G} and the PU_{10T-5G} ; this is expressed as follows (Othmane et al., 2020; Adardour et al., 2017):

$$\begin{aligned}
 \hat{d}_{(SU_{10T-5G}; PU_{10T-5G})} &= \\
 &= \sqrt{(x_i(PU_{10T-5G}) - x_i(SU_{10T-5G}))^2 + (y_j(PU_{10T-5G}) - y_j(SU_{10T-5G}))^2}
 \end{aligned} \quad (3)$$

Where, the coordinates $(x_i(SU_{10T-5G}), y_j(SU_{10T-5G}))$ of SU_{10T-5G} are derived through GMRMM and the coordinates $(x_i(PU_{10T-5G}), y_j(PU_{10T-5G}))$ of PU_{10T-5G} are set to $(0,0)$.

2.2.2 RSS_{5G} at the SU_{10T-5G} under LNS model: The estimated RSS_{5G} in [dB] from PU_{10T-5G} to SU_{10T-5G} is derived as follows (Othmane et al., 2020; Adardour et al., 2017):

$$\hat{P}_r(SU_{10T-5G}) = P_{t(PU_{10T-5G})} - \left(PL_0 + 10 \cdot PLE_{(LOS/NLOS)} \cdot D_{\hat{d}/d_0} \right) \quad (4)$$

Where,

$$D_{\hat{d}/d_0} = \log_{10} \left(\frac{\hat{d}_{(SU_{10T-5G}; PU_{10T-5G})}}{d_0} \right) \quad (5)$$

It is assumed from equation (3) that the Log-Distance Path Loss (or LDPL) model is characterized as follows:

$$\left[\frac{\hat{P}_r(SU_{10T-5G})}{\hat{P}_r(SU_{10T-5G})(d_0)} \right]_{[dB]} = -10 \cdot PLE_{(LOS/NLOS)} \cdot D_{\hat{d}/d_0} \quad (6)$$

$$\hat{P}_r(SU_{10T-5G})(d_0) = P_{t(PU_{10T-5G})} - PL_0 \quad (7)$$

$$PL_0 = 20 \cdot \log_{10} \left(\frac{4\pi d_0}{\lambda} \right) \quad (8)$$

On the other hand, in order to have the LNS effects model, one needs to add an auxiliary element $X_{\sigma(LOS/NLOS)}$ in the LDPL model, where the last model (6) given by the following form:

$$\left[\frac{\hat{P}_r(SU_{10T-5G})}{\hat{P}_r(SU_{10T-5G})(d_0)} \right]_{[dB]} = -10 \cdot PLE_{(LOS/NLOS)} \cdot D_{\hat{d}/d_0} + \dots + X_{\sigma(LOS/NLOS)} \quad (9)$$

Where, $\hat{P}_r(SU_{10T-5G})$, $P_{t(PU_{10T-5G})}$, PL_0 , $\hat{d}_{(SU_{10T-5G}; PU_{10T-5G})}$, λ and $PLE_{(LOS/NLOS)}$, are: the estimated RSS_{5G} at the SU_{10T-5G} in [dB], the transmitted PS_{5G} by the PU_{10T-5G} in [dB], the path loss based on a reference distance d_0 in [dB], the estimated distance

between the SU_{IoT-5G} and the PU_{IoT-5G} in [m], the wavelength of the PS_{5G} in [mm] and the path loss exponent in line-of-sight (or LOS) or none-line-of-sight (or, NLOS), respectively, and $X_{\sigma_{(LOS/NLOS)}}$ is a GD-RV (or Gaussian distributed-random variable) with zero mean and standard deviation ($\sigma_{(LOS/NLOS)}$) in [dB].

There is however a need to apply a reliable method to detect the estimated RSS_{5G} at the SU_{IoT-5G} which is considered more stable in a congested environment. For this purpose, a simple recursive estimator (or SRE) is applied, as depicted in the formula below:

$$\bar{P}_{r(SU_{IoT-5G})}(t) = [\delta \cdot \hat{P}_{r(SU_{IoT-5G})}(t)] + \dots \\ \dots + [(1 - \delta) \cdot \bar{P}_{r(SU_{IoT-5G})}(t - 1)] \quad (10)$$

Where, $\delta(0 < \delta \leq 1)$ is the weighting factor (Othmane et al., 2020; Adardour et al., 2017).

2.2.3 SNR sensitivity under LNS model : The sensitivity estimation of the $\overline{SNR}_{(SU_{IoT-5G}; PU_{IoT-5G})}$ for the link between two nodes the SU_{IoT-5G} and the PU_{IoT-5G} is performed as follows (Adardour et al., 2017; Othmane et al., 2020):

$$\overline{SNR}_{(SU_{IoT-5G}; PU_{IoT-5G})}[dB] = \frac{\bar{P}_{r(SU_{IoT-5G})}}{N_{Power}} \quad (11)$$

$$\overline{SNR}_{(SU_{IoT-5G}; PU_{IoT-5G})}[dB] = 10 \log_{10} \left(\frac{\bar{P}_{r(SU_{IoT-5G})}}{N_{Power}} \right) \quad (12)$$

2.3 Simple Energy Detector

In this subsection, the local detection (or LD) model of PS_{5G} is introduced. However, the spectrum sensing method about 60 GHz frequency band or APWLAN_{*IoT-5G*} (or PU_{IoT-5G}) is very simple, which is divided into two cases: the local detection (or LD) of PS_{5G} and the cooperative detection (or CD) of PS_{5G} . In this paper, the LD method of PS_{5G} around the 60 GHz frequency is exploited. Nevertheless, it is considered that the SU_{IoT-5G} features an energy detector to detect the PS_{5G} in order to authenticate whether the PU_{IoT-5G} is available or not in WLAN_{*IoT-5G*} area. It may be summarized as follows (Adardour et al., 2015; Othmane et al., 2020):

- The estimated RSS_{5G} at the SU_{IoT-5G} is indicated as follows if the APWLAN_{*IoT-5G*} is not available:

$$Y_{\bar{P}_{r(SU_{IoT-5G})}}(t) = N_{AWGN}(t) \rightarrow H_0 \quad (13)$$

- When the APWLAN_{*IoT-5G*} is available, the estimated RSS_{5G} at the SU_{IoT-5G} is indicated as follows:

$$Y_{\bar{P}_{r(SU_{IoT-5G})}}(t) = S_{P_t(PU_{IoT-5G})}(t) + N_{AWGN}(t) \rightarrow H_1 \quad (14)$$

Where, $Y_{\bar{P}_{r(SU_{IoT-5G})}}$ is the estimated RSS_{5G} at the SU_{IoT-5G} , $S_{P_t(PU_{IoT-5G})}(t)$ is the PS_{5G} from the APWLAN_{*IoT-5G*} and $N_{AWGN}(t)$ is the additive white Gaussian noise (or AWGN). Based on the observation of $Y_{\bar{P}_{r(SU_{IoT-5G})}}(t)$, the SU_{IoT-5G} needs to reach a decision between H_0 (APWLAN_{*IoT-5G*} is not available) and H_1 (APWLAN_{*IoT-5G*} is available).

Assuming that $E_{Y_{\bar{P}_{r(SU_{IoT-5G})}}}$ is the observed energy of $Y_{\bar{P}_{r(SU_{IoT-5G})}}$, it may be expressed as:

$$E_{Y_{\bar{P}_{r(SU_{IoT-5G})}}} = \left(\frac{1}{M} \right) \sum_{n=1}^M \left| Y_{\bar{P}_{r(SU_{IoT-5G})}} \right|_n^2 \quad (15)$$

Where, $Y_{\bar{P}_{r(SU_{IoT-5G})}}$ refers to a sample obtained from the estimated RSS_{5G} at the SU_{IoT-5G} and $M = 2 \cdot T \cdot W$ refers to the total number of samples. Then, the estimated RSS_{5G} at the SU_{IoT-5G} is detected in a bandwidth W within an observation time T .

Moreover, the output energy $E_{Y_{\bar{P}_{r(SU_{IoT-5G})}}}$ of a detector (i.e., SU_{IoT-5G}) is partitioned as follows:

$$\begin{cases} E_{Y_{\bar{P}_{r(SU_{IoT-5G})}/H_0}} = \left(\frac{1}{M} \right) \sum_{n=1}^M |N_{AWGN_n}|^2 \\ E_{Y_{\bar{P}_{r(SU_{IoT-5G})}/H_1}} = \left(\frac{1}{M} \right) \sum_{n=1}^M \left| S_{P_t(PU_{IoT-5G})}_n + N_{AWGN_n} \right|^2 \end{cases} \quad (16)$$

It is possible to write the formula (16) as follows:

$$\begin{cases} E_{Y_{\bar{P}_{r(SU_{IoT-5G})}/H_0}} = \chi_M^2 \\ E_{Y_{\bar{P}_{r(SU_{IoT-5G})}/H_1}} = \chi_M^2(2 \cdot \gamma) \end{cases} \quad (17)$$

Where, $\gamma = \overline{SNR}_{(SU_{IoT-5G}; PU_{IoT-5G})}$ in [dB], χ_M^2 and $\chi_M^2(2 \cdot \gamma)$ display the central and non-central Chi^{square} distributions with M degrees of freedom, respectively [42,44].

The sensing performances of PS_{5G} in WLAN_{*IoT-5G*} under an AWGN channel are discussed through two measures: Probability of Detection (or PD) and Probability of False Alarm (or PFA), which are equivalent to [42,44]:

$$PD = Prob \left(E_{Y_{\bar{P}_{r(SU_{IoT-5G})}}} > E_{Th} | H_1 \right) \\ PD = Q_M \left(\sqrt{2 \cdot \overline{SNR}_{(SU_{IoT-5G}; PU_{IoT-5G})}} \cdot \sqrt{E_{Th}} \right) \quad (18)$$

$$PFA = Prob \left(E_{Y_{\bar{P}_{r(SU_{IoT-5G})}}} > E_{Th} | H_0 \right) = \frac{\Gamma(M, \frac{E_{Th}}{2})}{\Gamma(M)} \quad (19)$$

Where, $\Gamma(\cdot)$ and $\Gamma(\cdot, \cdot)$ are complete and incomplete gamma functions, respectively. $Q_M(\cdot, \cdot)$ is the generalized Marcum Q -function and E_{Th} is the threshold energy for decision-making?

Yet, the Probability of Total Detection Error (or PTED) of PS_{5G} at 60 GHz from the APWLAN_{*IoT-5G*} can be derived from the following formula (20) (Adardour et al., 2015; Othmane et al., 2020):

$$PTED = PMD + PFA \quad (20)$$

Where, PMD is the Probability Missing Detection of PS_{5G} at 60 GHz from the APWLAN_{*IoT-5G*}.

3. SIMULATION AND RESULTS

3.1 Simulation setup

In this part, the computer simulations have been performed using MATLAB R2017a software. The aim of the current work is to improve the sensing performances of APWLAN_{*IoT-5G*} (or PS_{5G} at 60 GHz) in a real-time WLAN_{*IoT-5G*}, taking into account that the environment of the WLAN_{*IoT-5G*} is congested, together with considering the mobility impact of the SU_{IoT-5G} for three proposed scenarios, see Table 2. The considered parameters in our experiments are given in Table 3 (Sun et al., 2016; Joongheon et al., 2017; Zhang and Yu, 2019).

	Propagation model	Observation channel
Scenario (A)	Free space trajectory loss (or FSTL)	AWGN
Scenario (B)	LNS (PLE _(LOS))	AWGN
Scenario (C)	LNS (PLE _(NLOS))	AWGN

Table 2. PS_{5G} sensing scenarios in WLAN_{IoT-5G}.

Parameters	Values
WLAN _{IoT-5G} model	50 x 50 [m ²]
Frequency	60 [GHz]
Transmission power of APWLAN _{IoT-5G}	15 [dBm]
Noise power at SU _{IoT-5G}	-139 [dBm]
Path loss exponent	PLE _(LOS) = 2.17 and PLE _(NLOS) = 3.01
Reference distance	1.0 [m]

Table 3. Simulation parameters.

3.2 Results and interpretations

In this work, the first steps of our algorithms (see Fig. 1) aimed to estimate the RSS_{5G} at the SU_{IoT-5G} as well as the sensitivity estimation of the $\overline{SNR}(SU_{IoT-5G}; PU_{IoT-5G})$ between the APWLAN_{IoT-5G} and the SU_{IoT-5G}. To do this, we first estimate the trajectory of SU_{IoT-5G} with reference to a landmark that will be the APWLAN_{IoT-5G} position, and then the velocity of the SU_{IoT-5G} using the GMRMM.

However, the SU_{IoT-5G} movement within the WLAN_{IoT-5G} for the three proposed propagation models (see Table 2) is depicted in Fig. 2. The SU_{IoT-5G} starts its movement at the point $(\sqrt{2}, \sqrt{2})$ and moves along time for $t = 200$ s; the distance d between the SU_{IoT-5G} initial position (i.e., yellow point) and the APWLAN_{IoT-5G} (i.e., red triangle) is 1.0 m. Furthermore, to carry out this motion, the following GMRMM parameters are defined, namely the time interval as 1.0 s, $\alpha = 0.0075$, $\vec{V}_{SU_{IoT-5G}} = 0.3$ m/s and $\vec{D}_{SU_{IoT-5G}}$ initially is 45°. As shown in Fig. 2, the SU_{IoT-5G} is positioned in a closed environment of 130 x 130 [m²], as indicated by the dashed green square boundary, and the two black square contours are considered as obstacles in WLAN_{IoT-5G}. Moreover, it is very evident that the SU_{IoT-5G} follows a semi-random trajectory (see the zoom section of Fig. 2).

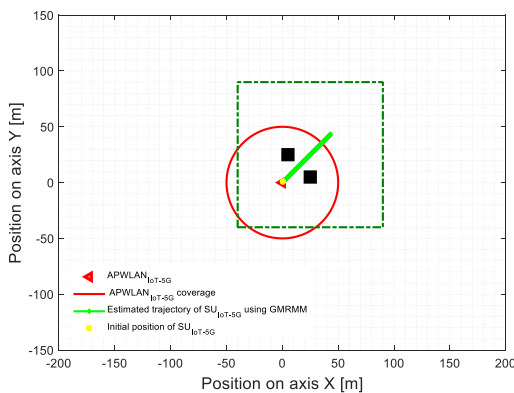


Figure 2. Estimated trajectory of SU_{IoT-5G} using GMRMM.

On the other hand, the estimated speed of SU_{IoT-5G} using the GMRMM algorithm is depicted in Fig. 3. Though, the movement speed per unit time of SU_{IoT-5G} in the WLAN_{IoT-5G} is shown in Fig. 3. Hence, one can clearly see that the speed decreases from $t = 1$ s with $V_{SU_{IoT-5G}(1s)} = 1.21$ m/s to $t = 108$ s with $V_{SU_{IoT-5G}(108s)} = 0.3105$ m/s. In addition, it should be noted that between the time $t = 109$ s and $t = 200$ s, the average

movement speed of SU_{IoT-5G} (or $V_{SU_{IoT-5G}(109s\ to\ 200s)}$) is equal to 0.3050 m/s. Consequently, the SU_{IoT-5G} speed remains relatively constant during the time interval from 109 s to 200 s.

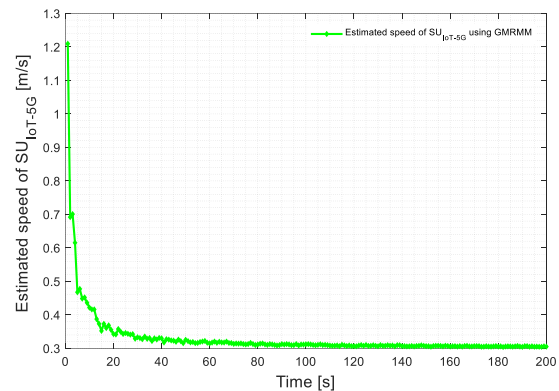


Figure 3. Estimated speed of SU_{IoT-5G} vs. Time [s].

In Figs. 4 and 5, the RSS_{5G} at the SU_{IoT-5G} and the sensitivity of the $\overline{SNR}(SU_{IoT-5G}; PU_{IoT-5G})$ between the APWLAN_{IoT-5G} and the SU_{IoT-5G} are illustrated for the three proposed scenarios (see Table 2). The RSS_{5G} value is estimated using the proposed algorithm, as seen in Fig. 4. From the Fig. 4, it is obvious that as the SU_{IoT-5G} moves to the extreme end of the radiation coverage area for WLAN_{IoT-5G}, which is far from the APWLAN_{IoT-5G}, the RSS_{5G} at the SU_{IoT-5G} is weaker.

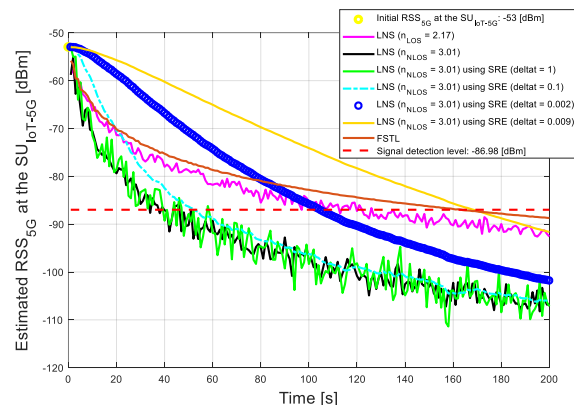


Figure 4. Estimated RSS_{5G} at the SU_{IoT-5G} vs. Time [s].

Throughout this step a Simple Recursive Estimator (or SRE) is employed. However, the SRE performance has been examined by the impact of the appropriate value of δ (delta) to correctly estimate the RSS_{5G} at the SU_{IoT-5G}; one has observed that δ is strongly correlated with the RSS_{5G} variation. Furthermore, one can clearly note that the fluctuation of the RSS_{5G} values at the SU_{IoT-5G} may be considered quite large when no average may be taken into account, i.e., when the δ value is equal to 1. Conversely, when the δ value is equal to 0.1, 0.02, and 0.009, the estimation of the RSS_{5G} at the SU_{IoT-5G} is absolutely acceptable. It is important, however, to achieve better stability for the RSS_{5G} at the SU_{IoT-5G}. To meet this goal, one can see that when averaging is applied with the δ value equal to 0.009, the RSS_{5G} values at the SU_{IoT-5G} are not so sensitive to rapid changes in terms of fluctuation.

According to step one and two of the proposed algorithm, it is possible to estimate the sensitivity of the received $\overline{SNR}(SU_{IoT-5G}; PU_{IoT-5G})$ at the SU_{IoT-5G}. From the obtained results as indicated in Fig. 5, one can easily observe that as SU_{IoT-5G}

moves further away from APWLAN_{IoT-5G} (refer to Fig. 2), the RSS_{5G} at the SU_{IoT-5G} is weaker (refer to Fig. 4); the sensitivity of the received $\overline{SNR}_{(SU_{IoT-5G}; PU_{IoT-5G})}$ at the SU_{IoT-5G} is also significantly weaker. As is illustrated in Fig. 5, one can see that the sensitivity estimation of the received $\overline{SNR}_{(SU_{IoT-5G}; PU_{IoT-5G})}$ at the SU_{IoT-5G} has the best performance when the δ value is equal to 0.009. In fact, δ is dependent on the shadowing parameter σ . One can notice that the proposed algorithm is less sensitive to fast variations of the sensitivity estimation of the received $\overline{SNR}_{(SU_{IoT-5G}; PU_{IoT-5G})}$ at the SU_{IoT-5G}, when an average $\delta = 0.009$ is applied. Therefore, it is important to obtain a stable estimate to increase the reliability of the PS_{5G} sensing performances at 60 GHz frequency.

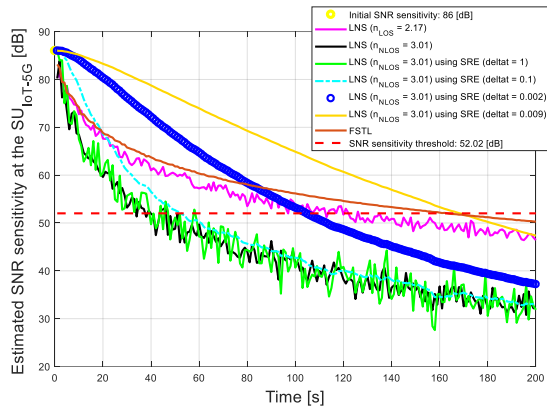


Figure 5. Estimated SNR sensitivity at the SU_{IoT-5G} vs. Time [s].

Based on the proposed algorithm, the objective of the second phase consists to estimate the PS_{5G} sensing level. The obtained results for the PTDE of PS_{5G} at 60 GHz frequency, are presented in Fig. 6, considering that the SU_{IoT-5G} moves within the radiation coverage area for WLAN_{IoT-5G}. In addition, the selected PFA is 10^{-6} .

3.2.1 Impact of SU_{IoT-5G} mobility on the PS_{5G} sensing performances at 60 GHz frequency: Considering the previous results obtained in the first phase, one can see that there is a clear influence on the PS_{5G} sensing performances at 60 GHz frequency for the three proposed scenarios (see Table 2), see Fig. 6 which gives the PTDE results. It is worth noting that when the sensitivity of the received $\overline{SNR}_{(SU_{IoT-5G}; PU_{IoT-5G})}$ at the SU_{IoT-5G} degrades, the PTDE of PS_{5G} at 60 GHz frequency is also increased. Therefore, the simple energy detector (or SED) performances which has been carried out by the SU_{IoT-5G} can also be significantly deteriorated.

3.2.2 Effectiveness of SRE on the PS_{5G} sensing performances at 60 GHz frequency: The SU_{IoT-5G} mobility in WLAN_{IoT-5G} and the PS_{5G} at 60 GHz frequency in a congested environment, have a noteworthy impact in the context of 5G spectrum sensing. Therefore, a SRE is suggested to improve the PS_{5G} (or APWLAN_{IoT-5G}) sensing performances at 60 GHz frequency.

After the analysis on the SRE use testing, the SRE provided us with some highlights for the proposed algorithm (see Fig. 1).

In the same context, the weighting factor δ impact on the PS_{5G} sensing performances is shown in Figs. 4 to 6. One can note that the simulation results are consistent with our goal. The sensing performances of PS_{5G} at 60 GHz frequency are significantly

improved in a congested environment, and especially for the third propagation model (see Table 2). It is also noted that varying the weighting factor δ has a significant positive impact on the PTDE (see Tables 4 and 5), confirming the importance of our contribution to the WLAN_{IoT-5G}.

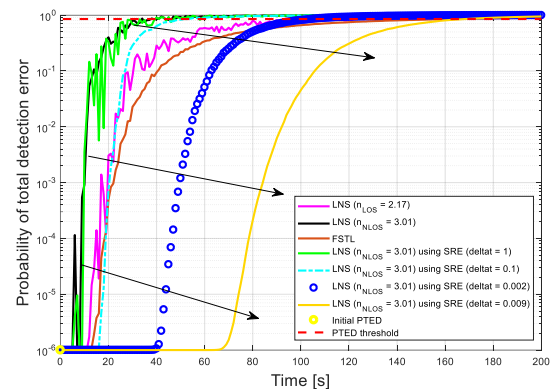


Figure 6. Probability of total detection error vs. Time [s].

Furthermore, it is clear from Fig. 6 and, Tables 4 and 5 that the minimum PTDE has been reached in the case where the weighting factor δ is equal to 0.009. Therefore, all three cases (i.e., the PTED for the three proposed scenarios in Table 2) have been compared with the estimated PTED, with $\delta = 0.009$.

δ	1	0.1	0.02	0.009
$\overline{SNR}_{(SU_{IoT-5G}; PU_{IoT-5G})}$ [dB]	35.87	38.55	45.33	57.15
$\overline{SNR}_{(SU_{IoT-5G}; PU_{IoT-5G})}$ threshold [dB]	52.02	52.02	52.02	52.02
PTED	0.9963	0.9928	0.9665	0.5948
PTED threshold	0.8529	0.8529	0.8529	0.8529

Table 4. Improved PTDE at t = 139 s, in third scenario.

at t = 139 s	$\overline{SNR}_{(SU_{IoT-5G}; PU_{IoT-5G})}$	PTED
Scenario (A)	53.37 dB	0.8046
Scenario (B)	50.54 dB	0.8929
Scenario (C)	34.34 dB	0.9973
Improved Scenario (C) / $\delta = 0.009$	57.15 dB	0.5948

Table 5. Sensing performances of a PS_{5G} at 60 GHz frequency in different scenarios.

4. CONCLUSION

This paper has presented an efficient algorithm to improve the sensing performances of primary signal 5G for WLAN_{IoT-5G} in a real-time, while the environmental impact and the SU_{IoT-5G} mobility are taken into account. However, the sensing reliability has been improved by the use of a simple recursive estimator. From the obtained results, it can be stated that the proposed algorithm can stabilize the received signal strength at the SU_{IoT-5G} in a congested environment for WLAN_{IoT-5G}, while achieving the minimum probability of total detection error of primary signal 5G around the 60 GHz frequency.

REFERENCES

Adardour, H.E., Meliani, M., and Hachemi, M.H., 2015. Estimation of the Spectrum Sensing for the Cognitive Radios:

- Test Analysing Using Kalman Filter, in *Wireless Pers Commun*, 84, 1535–1549. <https://doi.org/10.1007/s11277-015-2701-y>
- Adardour, H.E., Meliani, M., and Hachemi, M.H., 2017. Improved local spectrum sensing in cluttered environment using a simple recursive estimator, *Computers and Electrical Engineering* 61, July 2017, 208-222. <http://dx.doi.org/10.1016/j.compeleceng.2016.11.037>
- Azzahra, M. A., and Iskandar, 2018. Performance of 60 GHz Millimeter-Wave Propagation in Indoor Environment, in: 2018 International Symposium on Electronics and Smart Devices (ISESD), 2018, pp. 1-4, doi: 10.1109/ISESD.2018.8605447
- Geng, F., and Xue, S. 2013. A comparative study of mobility models in the performance evaluation of MCL. 2013 22nd Wireless and Optical Communication Conference, 2013, 288-292, doi: 10.1109/WOCC.2013.6676324.
- Herschfelt, A., Chiriyath, A. R., Srinivas, S., and Bliss, D. W., 2021. An Introduction to Spectral Convergence: Challenges and Paths to Solutions, in: 2021 1st IEEE International Online Symposium on Joint Communications & Sensing (JC&S), 2021, pp. 1-6, doi: 10.1109/JCS52304.2021.9376388
- Joongheon, K., Jae-Jin, L., and Woojoo, L., 2017. Strategic Control of 60 GHz MillimeterWave High-Speed Wireless Links for Distributed Virtual Reality Platforms, in *Hindawi, Mobile Information Systems*, Volume 2017, Article ID 5040347, 10 pages. <https://doi.org/10.1155/2017/5040347>
- Liang, B., and Haas, Z. J. 1999. Predictive distance-based mobility management for PCS networks. *IEEE INFOCOM '99, Conference on Computer Communications, Proceedings, Eighteenth Annual Joint Conference of the IEEE Computer and Communications Societies. The Future is Now (Cat. No.99CH36320)*, 3, 1999, 1377-1384. doi: 10.1109/INFCOM.1999.752157.
- Mohanty, S., Agarwal, A., Agarwal, K., Mali, S., and Misra, G., 2021. Role of Millimeter Wave for Future 5G Mobile Networks: Its Potential, Prospects and Challenges, in: 2021 1st Odisha International Conference on Electrical Power Engineering, Communication and Computing Technology (ODICON), 2021, pp. 1-4, doi: 10.1109/ODICON50556.2021.9429017
- Objetconnecte. net., 2022. <https://www.objetconnecte.com/5g-quel-impact-sur-linternet-des-objets-iot/> (Access date: 30/06/2022).
- Othmane, B., et Adnane, B.A. 2020. Estimation d'un signal primaire dans un réseau 5G par un utilisateur secondaire à base d'un détecteur d'énergie. End-of-study project (ESP) to obtain the Master degree in Telecommunications at the University of Tlemcen, 2020. <http://dspace.univ-tlemcen.dz/handle/112/15709>.
- Singh, H., Prasad, R. & Bonev, B. 2018. The Studies of Millimeter Waves at 60 GHz in Outdoor Environments for IMT Applications: A State of Art. *Wireless Pers Commun* 100, 463–474. <https://doi.org/10.1007/s11277-017-5090-6>
- Sun, S., et al., 2016. Investigation of Prediction Accuracy, Sensitivity, and Parameter Stability of Large-Scale Propagation Path Loss Models for 5G Wireless Communications, in *IEEE Transactions on Vehicular Technology*, 65(5), 2843-2860, May 2016, doi: 10.1109/TVT.2016.2543139
- Tracy C, Jeff B, Vanessa D. A Survey of Mobility Models for Ad Hoc Network Research. *Wireless Communication & Mobile Computing (WCMC): Special issue on Mobile AdHoc Networking: Research, Trends and Applications 2002*; 2, 483–502. <https://doi.org/10.1002/wcm.72>
- Xiaoyan, H., Mario, G., Guangyu, P., and Ching-Chuan, C. 1999. A group mobility model for ad hoc wireless networks. In *Proceedings of the 2nd ACM international workshop on Modeling, analysis and simulation of wireless and mobile systems (MSWiM '99)*. Association for Computing Machinery, New York, NY, USA, 53–60. <https://doi.org/10.1145/313237.313248>.
- Zhang, Z., and Yu, H., 2019. Beam interference suppression in multi-cell millimeter wave communications, in *Digital Communications and Networks*, 5(3), 196-202, <https://doi.org/10.1016/j.dcan.2018.01.003>.